Desalination and Water Treatment
www.deswater.com

doi: 10.5004/dwt.2023.30112

314 (2023) 276–285
December

Biosorption study of basic dye using aerial part of widely growing weed *Chenopodium album*

Nidhi Rai[a], Durgesh Kumar Sinha[a], Sanju Soni[a], Santosh Kumar[a], Sadanand Sharma[b], Jyoti Mittal[c], Charu Arora[a,*]

[a]*Department of Chemistry, Guru Ghasidas Vishwavidyalaya, Bilaspur, C.G.-495009, India, emails: charuarora77@gmail.com/ charuarora150@gmail.com (C. Arora), needhirai786@gmail.com (N. Rai), durgesh2428@gmail.com (D.K. Sinha), sanjusoni87@gmail.com (S. Soni), santoshkumar06394@gmail.com (S. Kumar)*
[b]*Central Institute of Mining & Fuel Research (Council of Scientific & Industrial Research), Ministry of Science & Technology, Govt. of India, Barwa Road, Dhanbad-826015 (Jharkhand), India, email: sns2sangi1581@gmail.com*
[c]*Department of Chemistry, Maulana Azad National Institute of Technology, Bhopal, M.P., India, email: jyalmittal@gmail.com*

Received 8 October 2023; Accepted 28 October 2023

ABSTRACT

In the present study, the fine powder of the aerial part of the invasive weed *Chenopodium album* has been explored to effectively eliminate the organic dye Crystal violet from its water solution. The fine powder of the aerial part of the weed has been characterized by scanning electron microscopy, X-ray diffraction and Fourier-transform infrared spectroscopy techniques. Its impact on various parameters of dye elimination has been investigated. It is found that the magnitude of adsorption is greater at pH 8 and increases with temperature. Different adsorption isotherms and kinetic models were employed to match the adsorption methods data. The data successfully fit the Freundlich, Hill adsorption model and interparticle models with R^2 values of 0.99, 0.99 and 0.97, respectively. The adsorption capacity of *C. album* based biosorbent was greater in batch experiments in comparison to bulk-using column operations. The biosorbent made of *C. album* can be used as a robust material for removing the dye Crystal violet. The bio-adsorbent used in the present study has exhibited much better efficiency (Q_e = 219.4 mg/g) in comparison to the ash of the *C. album* employed for the adsorption of Crystal violet dye.

Keywords: Chenopodium album; Bio adsorbent; Crystal violet

1. Introduction

The untreated discharge of industrial effluents has intensified the scarcity of clean water in the whole world. Developing countries, like India, are facing more issues due to unrestrained population progress and the application of several old-fashioned practices and equipment that consume a lot of water in both agricultural and industrial operations. Different industries like paper, textile, leather, etc. use poisonous chemicals to produce completed projects, and the fallow portion of it outflows into the surrounding area as trash from industry [1]. Researchers worldwide are trying to develop inexpensive and competent technologies for the cleaning of sewage water. The main contaminants in industrial effluents are phenolics, poisonous metals, and dyes even at minimal amounts, these have adverse impacts on the environment. Dyes are the most tarnished organic contaminants as they are water-soluble and dispersible. Crystal violet (CV) is one the most popular dye that is released from paper, textile, cosmetics, and analytical chemistry/biochemistry. CV concentrations in industrial effluents have been shown to range from trace quantities to 150 mg/L, depending on the

---

* Corresponding author.

specific usage [2]. CV has been shown in toxicological studies to have cancer-causing and mutagenic effects in animals. It could cause digestive tract and digestive system irritation, as well as long-term corneal and conjunctival damage. In severe cases, it may result in kidney and respiratory failure as well as lifelong blindness. When this dye-containing water is discharged into water bodies, the environment can be harmed and the dye is turned into leucon moiety [3–6]. Adsorptive removal of pollutants, as compared to other approaches like coagulation, chemical separation of membranes, oxidation, and electrochemical treatment method, is a simple and affordable way of cleaning dye-contaminated sewage water. A few research have been done on the elimination of organic and inorganic impurities, from wastewater using natural biosorbents, synthesized nanomaterials, and layer-altered substances, such as bottom ash, de-oiled soya, and hen feather [7–17]. CV dye was removed from its aqueous medium by using some following adsorbents which are magnetic chitosan nanocomposites (MCNCs), carboxylated activated carbon (CAC) which was prepared by organochlorine compound and sodium hydroxide, modified sugarcane bagasse modified with Meldrum's acid, novel bio-nanocomposite (Alg-Cst/Kal), and cross-linked chitosan coated bentonite (CCB) beads under acidic condition [18–22]. Adsorption has proven to be a very effective and widely used method to clean savage water in the textile industry because it is a process that can be economically used to remove the dye and decolorize textile effluents. The interaction between the adsorbent and dye, as well as the surface area of the adsorbent, particle size, pH, time of contact, and temperature, are the key parameters that affect dye adsorption. Adsorption is one of many techniques used for dye elimination studies. Others include the degradation of chemicals in the presence of photo light, oxidation of chemical substances, advanced oxidation process (AOP), degradation of biological substances, coagulation, reverse osmosis, flotation, electrochemical studies, etc [23–29]. Due to its efficiency and reusability adsorption is mostly preferred over alternative approaches for the elimination of dyes from water. For the elimination of dye from its water solutions, a variety of adsorbents have been utilized.

Chenopodium album is a rapid-sprouting weedy genus of annual plants of *Chenopodium* and has 250 species worldwide. Twenty-one species are found in India; mostly cultivated to use as vegetables and a few for grains. The young plant can be used as food and herbal medicine [30]. *C. album* is thought to be a potential wild vegetable worth exploring and utilizing [31]. It is a multifaceted erect plant that can be grown to 3.5 cm tall. The traditional uses of *C. album* (manure weed) include anthelmintics, cardiotonic, carminatives, digestives, diuretics, and laxatives. It is also suitable for dyspepsia, peptic ulcer, strangury, flatulence, splenopathy, pharyngopathy, ophthalmopathy and general debility [32–35]. Along with medicinal properties, it shows the efficient elimination of heavy metals from aqueous waste. Manure ash after chemical modification can be applied for the elimination of dye from their water solution [36]. The potential for eliminating CV from its solution using the *C. album* areal part, which was crushed to powder form, was investigated in the current work. Effect of various parameters viz. temperature, initial dye concentration, pH, dose, and contact time were some of the parameters whose effects were assessed. Kinetics and equilibrium adsorption data were used to analyse the adsorption process. To explore dye removal by *C. album* powder in the current work, both batch and column methods were explored.

2. Materials and method

2.1. Chemical reagents

The dye CV was bought from Merck M/s, India. The hydrochloric acid and sodium hydroxide used to maintain the solution pH were purchased from CDH Fine Chemicals M/s, India. The stock solution of 100 g/mL was prepared using deionized water further it was diluted to carry out batch and column studies.

2.2. Development of adsorbent

Areal part of the *C. album* was procured from Bilaspur, Chhattisgarh, India. It was sun-dried for many hours after that it was ground and sieved. The powder of *C. album* root was used without any chemical treatment.

2.3. Physical and chemical characterizations

Scanning electron microscopy (SEM) micrographs of the adsorbent acquired with the Merlin VP Compact (Carl Zeiss, Germany) before adsorption were used to examine the surface morphology. Adsorbent's functional groups were detected via Fourier-transform spectroscopy using a Nicolet iS10, Thermo Fisher Scientific Instrument, Madison, USA, OMNIC 9. Shimadzu UV-1800 Spectrophotometer was used to quantify the concentration of CV dye used in the experiment. All experiments were carried out at 589 nm ($\lambda_{\max}$).

2.4. Dye removal experiments

Adsorption of CV from aqueous solution by the fine powder of aerial part of *C. album* was studied by batch techniques. 50 mL of CV dye are taken out for each concentration 10–120 mg/L for a batch experiment. HCl (1 M) and NaOH (1 M) solutions were employed to investigate the effect of pH. Different parameters were studied for the experiment for instance a contact time range 0–540 min, adsorbent dose 15–40 mg, and temperature 30°C–55°C. The solution of different pH ranged from 3 to 11. The concentration of CV was monitored on a spectrophotometer at 589 nm. Using the provided formulas, the percentage dye removal (R %), and the quantity of dye removed at equilibrium (q_e, mg/g) and at time t (q_t, mg/g), were all computed using Eqs. (1–3) [37].

$$q_e = \frac{\left(C_0 - C_e\right)V}{M} \tag{1}$$

$$q_t = \frac{\left(C_0 - C_t\right)V}{M} \tag{2}$$

$$R\left(\%\right) = \frac{\left(C_0 - C_e\right)}{C_0} \times 100 \tag{3}$$

where C_0 (mg/L) and C_e (mg/L) are the initial and equilibrium dye concentrations, respectively. q_t signifies the amount of dye absorbed at equilibrium between the adsorbent and q_e.

Mass transfer mechanisms include adsorption that causes the deposition of material at the boundary of the adsorbent and aqueous solution of dye. The interactions of adsorbent and adsorbate are characterized by sorption isotherms, which typically depict the ratio between the amount that is adsorbed and that which is still in the aqueous solution at equilibrium at a constant temperature. Several isotherm models are explored to fit the isotherm data to generate a model to be utilized in to design process. The adsorption treatments results were averaged from three duplicate samples, and analysis of the control samples was done on those samples as well. Linear Eqs. (4)–(7), respectively, express the Langmuir, Freundlich, Temkin isotherms and non-linear Hill adsorption model [15,38]:

$$\frac{C_e}{Q_e} = \frac{1}{K_L Q_L} \frac{C_e}{Q_L} \tag{4}$$

$$\ln q_e = \ln K_f + \frac{1}{n}\left(\ln C_e\right) \tag{5}$$

$$Q_e = \frac{RT}{b_T}\ln K_T + \frac{RT}{b_T}\ln C_e \tag{6}$$

$$q_e = \frac{q_{\mathrm{SH}} C_e^{n_H}}{K_D + C_e^{n_H}} \tag{7}$$

The dye solution equilibrium concentration is C_e (mg/L) while Q_e (mg/g) is the quantity of dye absorbed by a sorbent at equilibrium. K_f and n, K_L and Q_L, b_T and K_T, K_D, n_H and q_H are constants that cover factors impacting the sorption mechanism for the Freundlich, Langmuir, Temkin and Hill isotherm model, respectively. K_f and $1/n$, respectively, represent the sorption capacity and surface heterogeneity in a Freundlich model. Q_L and K_L stand for, adsorption capacity and energy, respectively for the Langmuir model. The equilibrium binding energy in the Temkin isotherm is defined by the Temkin constant (b_T) [39,40].

2.5. Kinetics and thermodynamics study

Information on mass transfer processes, adsorbent performance, and adsorption rate is provided through adsorption kinetic studies. We have explored pseudo-first-order, pseudo-second-order, and interparticle diffusion models in the current investigation to help make sense of the experimental findings. The interparticle diffusion kinetics, pseudo-first-order and pseudo-second-order may be stated as:

$$\ln\left(Q_e - Q_t\right) = \ln Q_e - k_1 t \tag{8}$$

$$\frac{t}{Q_t} = \frac{t}{Q_e} + \frac{1}{k_2 Q_e^2} \tag{9}$$

$$Q_t = k_i t^{1/2} + C \tag{10}$$

where k_1 (min^{-1}), k_2 (g/mg·min) and k_i stand for first-order, second-order and interparticle diffusion rate constants, respectively. The border effect and C in the interparticle diffusion model are connected.

Interpreting the equations to determine the adsorption mechanism, all related thermodynamic parameters were assessed using Eqs. (11) and (12).

$$\ln K = \frac{-\Delta H^\circ}{RT} - \frac{\Delta S^\circ}{R} \tag{11}$$

$$\Delta G^\circ = RT \ln K_c \tag{12}$$

where K_c is the adsorption equilibrium constant and other constants have the usual meaning [41].

2.6. Column adsorption

Using a fixed bed adsorber, the majority of the dye was continuously removed. The column study was run in a glass column of a height of 19 and 1 cm interior width and a 0.9 cm bed height. The amount of adsorbent used for fixed height was 500 mg on a cotton wool support. The amount of dye concentration used was 500 ppm, flow rate of 2.5 mL/min. The sample (7.5 mL) was collected every 3 min for taking absorbance. A graph depicting the ratio C_t/C_0 as a function of time, where C_0 and C_t represent the initial effluent concentration and concentration at time t, respectively, serves as a representation of the breakthrough curve. The amount of dye adsorbed at time t is represented by the area under the breakthrough curve; integration will yield Q_{total} (mg). (Calculated using Software OriginPro 8) [36].

$$Q_{\mathrm{total}} = \upsilon \int_{t=0}^{t=t} \left(C_0 - C_t\right) dt \tag{13}$$

The quantity of dye transmitted to the column in total (m_{total}) at time t may be estimated using:

$$m_{\mathrm{total}} = C_0 \upsilon t \tag{14}$$

Percent dye removal R (%):

$$R = \frac{Q_{\mathrm{total}}}{m_{\mathrm{total}}} \times 100 \tag{15}$$

Dye adsorbed q_t (mg/g) at time t (Calculated Using Software OriginPro 8).

$$q_t = \frac{\upsilon \int_{t=0}^{t=t} \left(C_0 - C_t\right) dt}{m} \tag{16}$$

where m represents the amount of adsorbent utilized in the column [42].

3. Results and discussion

3.1. Characterization of adsorbent

The active groups and bonds found in plant materials are what cause their adsorption pattern. By using

Fourier-transform infrared spectroscopy, the functional group contained in the adsorbent is examined and the result obtained is shown in Fig. 1. As shown in Fig. 1 the aerial part of *C. album* has various peaks in 450–4,000 cm^{-1} range. Two significant band stretches can be seen in the area between 2,600 and 3,600 cm^{-1}. From 3,000 to 3,600 cm^{-1}, a strong and wide band stretch was seen, indicating alcohols, phenols, and carboxylic acids, which are present in pectin, cellulose, and lignin, were present on the surface of the adsorbent. The light stretching at 2,927 cm^{-1} is due to asymmetric or symmetric C–H vibration of aliphatic acids. The peak observed at 1,640 cm^{-1} is due to the alkene present in the plant sample. The symmetric stretching of pectin's –COO group may be responsible for the peaks at 1,384 cm^{-1}. The vibrating peaks of C–OH of the alcoholic and carboxylic group peak appears at 1,079 cm^{-1}. The surface morphology of the *C. album* aerial part was assessed by SEM image (Fig. 2). It reveals that the surface of powdered *C. album* consists of voids in it which is of the order of molecular size of CV dye. The average particle size of CV is 1.4 nm, and voids of *C. album* in SEM image have size of 1–1.5 μ, that is, 1,000 times larger than CV molecules, due to small size of CV, it easily gets trapped inside the voids present at the surface of *C. album*.

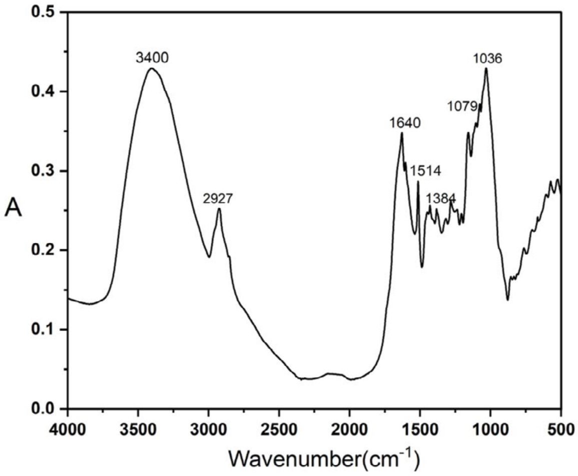

Fig. 1. Fourier-transform infrared spectrum of *Chenopodium album*.

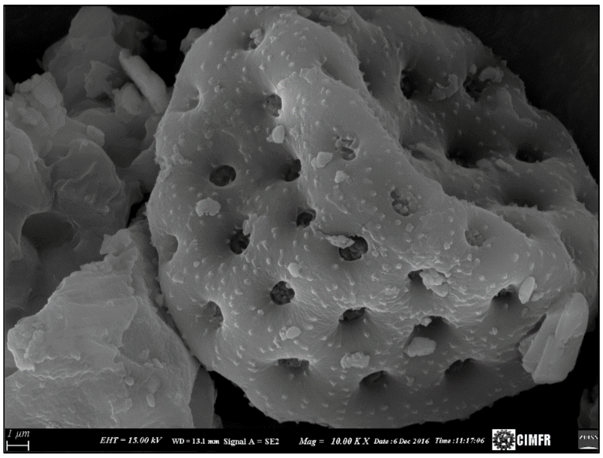

Fig. 2. Scanning electron micrograph of *Chenopodium album* aerial part.

3.2. Adsorption experiments

Influence of initial dye concentration and contact time.

An adsorbent dosage of 0.01 g at room temperature was used to investigate the effects of initial dye concentration and contact time on the sorption of CV on *C. album*. For this study, different concentration of CV was used (10–120 mg/L). From Fig. 3 it can be indicated that the dye elimination efficiency is higher for lower concentrations of CV and it increases with a rise in contact time. After 9 h the removal efficiency of 10 mg/L CV dye is 99% and for the higher concentration of CV (120 mg/L) the removal efficiency increases from 20% to 91% in 9 h. This could be possibly due to the initially large amount of vacant space obtainable in *C. album* so it shows better removal efficiency at lower concentrations of CV and with time more and more particles of CV get adsorbed on the adsorbent and this leads to an increase in removal efficiency with contact time. The highest amount of adsorption was discovered to be 77.12 mg/g.

3.3. Effect of dose

The optimization of the quantity of adsorbent is an essential phenomenon to study in batch adsorption study. Here we have executed the adsorption study by varying the amount from 15 to 40 mg and keeping the concentration of dye constant (40 mg/L). From Fig. 4 the elimination of dye improved as the amount of *C. album* powder increased because of an enhancement in the surface area and number of active sites. The maximum removal is shown at 40 mg (99.7%) after 9 h.

3.4. Influence of temperature

The adsorption process is influenced by the temperature. Adsorption experiments were performed at various

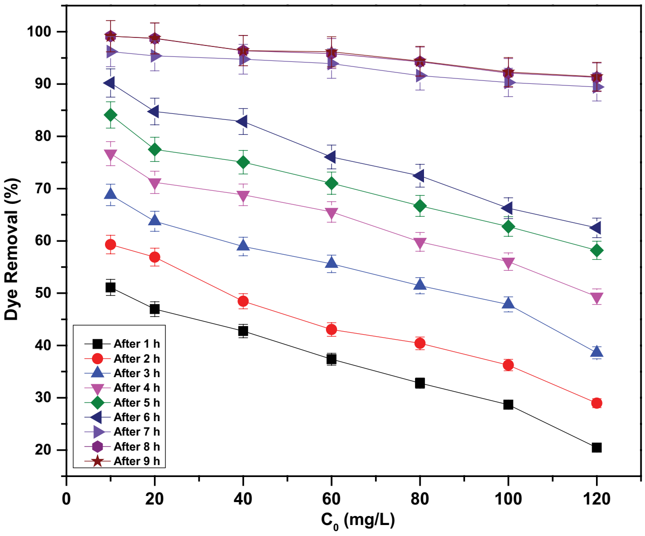

Fig. 3. Effect of initial dye concentration and contact time on Crystal violet adsorption by *Chenopodium album* at different time intervals.

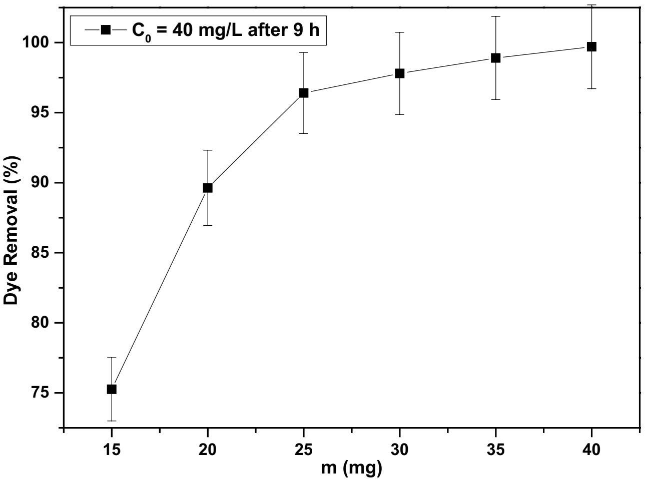

Fig. 4. Effect of dose of *Chenopodium album* on 40 mg/L Crystal violet dye solution after 9 h.

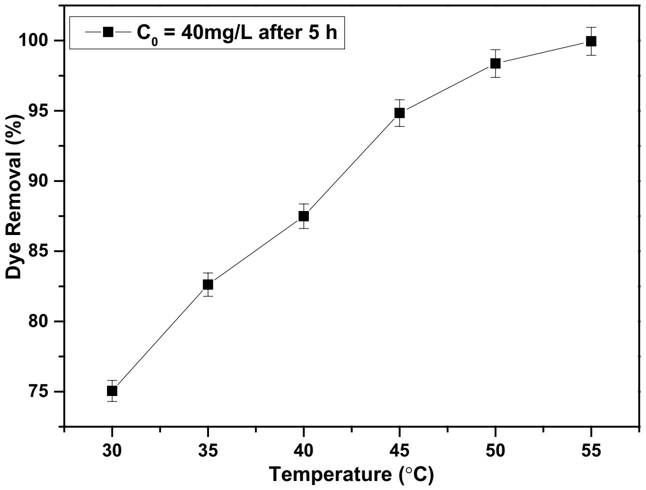

Fig. 5. Effect of temperature on 40 mg/L solution of Crystal violet adsorption by *Chenopodium album*.

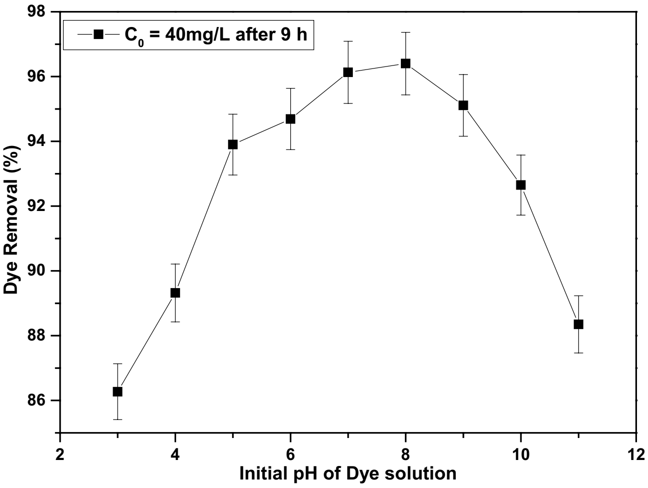

Fig. 6. Effect of pH on 40 mg/L solution of Crystal violet adsorption by *Chenopodium album*.

temperatures, viz. 303, 308, 313, 318, 323, and 328 K for 5 h contact duration. In these experiments, 10 mL of dye with a 40 mg/L concentration is adsorbed on 25 mg of adsorbent. Fig. 5 shows that the amount of dye removed increases with rising temperature. The removal efficiency increases from 75% to 99.7% on increasing temperature. Since there is a spike in the rate of dye molecule diffusion over external barriers and a decrease in solution viscosity, the equilibrium capacity of the adsorbent on adsorbate changes with temperature. This illustrates the endothermic nature of the adsorption [43].

3.5. Effect of pH

The solutions pH is crucial for the adsorption process. The degree of ionization of the dye molecule, as well as the surface charges of the adsorbent and adsorbate, are both regulated by the pH of the solution, which has a significant impact on adsorption effectiveness. The pH of the solution determines the type of interaction that occurs between the adsorbent and the adsorbate by causing ionization of solution species. Fig. 6 shows how the solutions initial pH, which ranges between 3–11, affects the adsorption capacity. As shown in Fig. 6, the adsorption capacity increases with increasing pH up to pH 8. The solution's elimination capacity rapidly declines as the pH is raised more. The highest amount of colour may be absorbed in pH 8 (96.4%). As the pH of the dye solution rises, the charge density decreases, reducing the electrostatic attraction between the positively charged dye molecule and the outermost layer of the adsorbent and increasing dye adsorption [44].

3.6. Adsorption equilibrium

The most common technique to interpret adsorption data, which employs the equilibrium isotherm value, plots the quantity of adsorbate removed per unit of sorbent as the sorbent's solid phase concentration vs. the amount of adsorbate in the liquid phase. The equilibrium isotherm value has a significant influence on the development and improvement of the adsorption for the elimination of a dye from its solution. As a result, finding the equilibrium curve needs correlation. A variety of isotherm models have been used to predict the authenticity of the data collected from experiments. In this study, the most widely used models—Langmuir, Freundlich, Temkin and Hill isotherms, were used to characterize the adsorption equilibrium. The monolayer adsorption of the dye molecule on the adsorbate surface is explained by Langmuir isotherm. Monolayer adsorption is the basis of the Langmuir isotherm, which occurs on an adsorbent with a homogenous structure, with all adsorption sites being equal and energetically equivalent. Specific homogenous sites inside the adsorbent are where adsorption takes place, once a dye molecule resides at a location, further adsorption cannot occur there [41]. It is projected that the adsorbate will be covered in a monolayer at the adsorbent's outside surface since the intermolecular forces diminish quickly with distance [44]. The exponential distribution of sites and their energy as well as the surface's variations are explained by the Freundlich isotherm. It is an empirical formula that governs multilayer adsorption.

The Temkin isotherm concept considers how indirect interactions between adsorbates might impact the adsorption process. Additionally, it assumes that the heat of adsorption for each molecule in the layer decreases linearly as the surface area does [42,45]. According to the Hill model, the adsorption process is a cooperative phenomenon, and the ability of a macromolecule to bind a ligand at one site may have an impact on other binding sites nearby [46,47].

From Figs. 7a–c and 8, a comparison of the Langmuir, Freundlich, Temkin and Hill adsorption isotherms showed that the sorption characteristics of CV dye onto *C. album* closely resembled the Freundlich and Hill isotherm equation. The closer to the unit value of their correlation coefficients (R^2) makes this conclusion much more encouraging. A forecast model's ability to accurately anticipate values and compare them to experimental data is shown by the correlation coefficient (R^2) [48]. Table 1 lists the CV on *C. album* adsorption parameters for the Langmuir, Freundlich, Temkin and Hill constants. The R^2 value was reported to be 0.942 for the Langmuir isotherm model, 0.992 for the Freundlich isotherm model, 0.899 and 0.990 for the Hill isotherm model. These observations suggest that the Freundlich and Hill isotherm equation, as opposed to the Langmuir and Temkin equation, provided a more accurate description of the adsorption of CV by *C. album*. This suggests that the process of adsorption was not simply monolayer but there was a formation of multilayer during the physical adsorption of CV onto the *C. album* [40,49,50].

3.7. Adsorption kinetics

The active groups and bonds present in plant materials are responsible for the adsorption pattern. Adsorption kinetic research defines the fast kinetics in aqueous phase adsorption. Pseudo-first-order, pseudo-second-order, and interparticle diffusion were employed to assess the kinetic data for this investigation. The Lagergren pseudo-first-order model was the first equation used to assess the kinetics data for the given system. In the analysis of kinetic data,

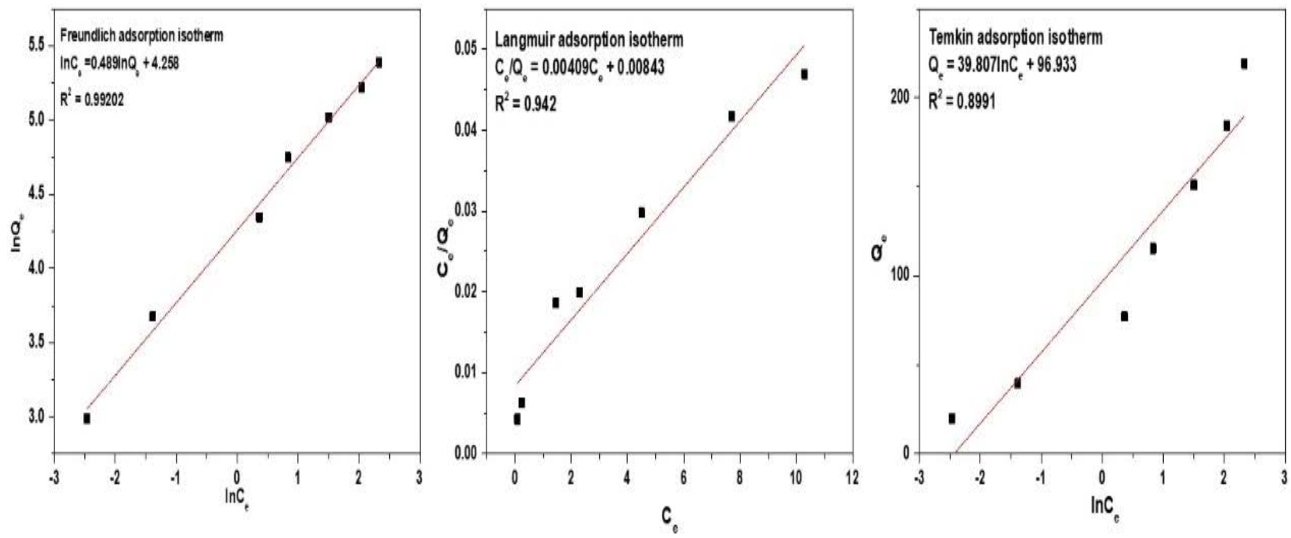

Fig. 7. Plots of studied adsorption isotherm models: (a) Freundlich adsorption isotherm, (b) Langmuir adsorption isotherm, and (c) Temkin adsorption isotherm.

Table 1
Adsorption isotherm parameters for adsorption of Crystal violet obtained through linear regression analysis of various isotherm models

Concentration of dye (mg/L)		Q_e (mg/g)	Freundlich isotherm			Langmuir isotherm			Temkin isotherm			Hill isotherm			
Initial	C_e	t	n	K_f	R^2	Q_L	K_L	R^2	b_T	K_T	R^2	q_m	K	η	R^2
10	0.085	19.83	2.04	3.78	0.99	2.02	118.62	0.94	65.52	11.36	0.89	1,702	22.62	0.51	0.99
20	0.25	39.5													
40	1.44	77.12													
60	2.3	115.4													
80	4.5	151													
100	7.7	184.6													
120	10.3	219.4													

kinetics models in linear form were employed. The model that best captured the kinetics and was used to show agreement between experimental data and the kinetic model yielding the highest R^2 value, is known as the correlation coefficient model [48,31]. The fitting charts of all explored kinetic models are depicted in Fig. 9a–c, and Table 2 provides an overview of all the outcomes. Using correlation coefficient data with $R^2 = 0.97322$, it is determined that the interparticle diffusion model fits better to the others. The value of R^2 for the pseudo-first-order and pseudo-second-order kinetics were calculated to be 0.62727 and 0.9525, respectively. Based on the available data, it was concluded that the present study exhibits chemisorption, with the electrostatic attraction between the molecules of the dye and the adsorbent serving as the mechanism [51].

3.8. Thermodynamic parameter

The process of adsorption is significantly influenced by temperature, which is seen by the quicker kinetics at higher temperatures. Based on mathematical Eqs. (11) and (12) [52], it is performed to evaluate the ΔG, ΔH, and ΔS thermodynamic parameters. Using the slope (H/R) and intercept (S/R) of the linear plot of $\ln(Q_e{\cdot}m/C_e)$ vs. $1/T$ (Fig. 10), the values of ΔH and ΔS were calculated, and the values of ΔG were calculated using Eqs. (11) and (12). Table 3 lists the values for the thermodynamics parameter. The ΔG value is negative for all six temperatures so the adsorption process will occur spontaneously. It has been found that as the temperature is raised, the value of ΔG rises, showing that the adsorption process is more favourable at higher

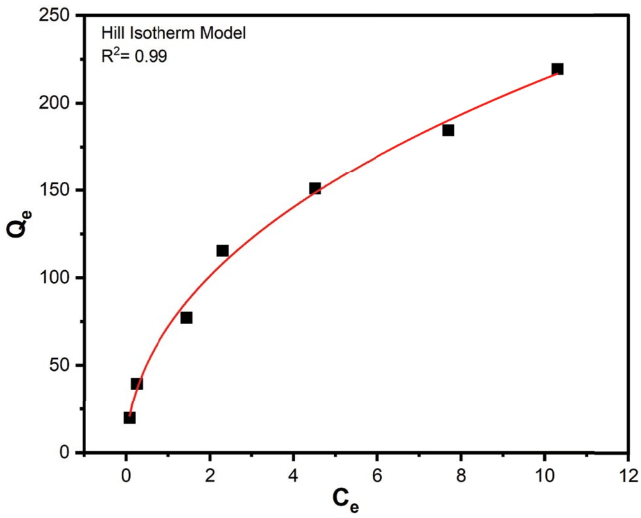

Fig. 8. Hill isotherm model.

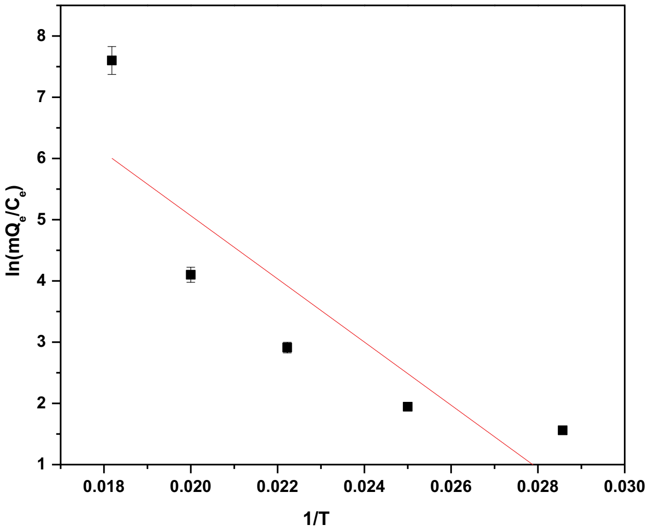

Fig. 10. Plot for thermodynamic parameter studies of adsorption of Crystal violet by *Chenopodium album*.

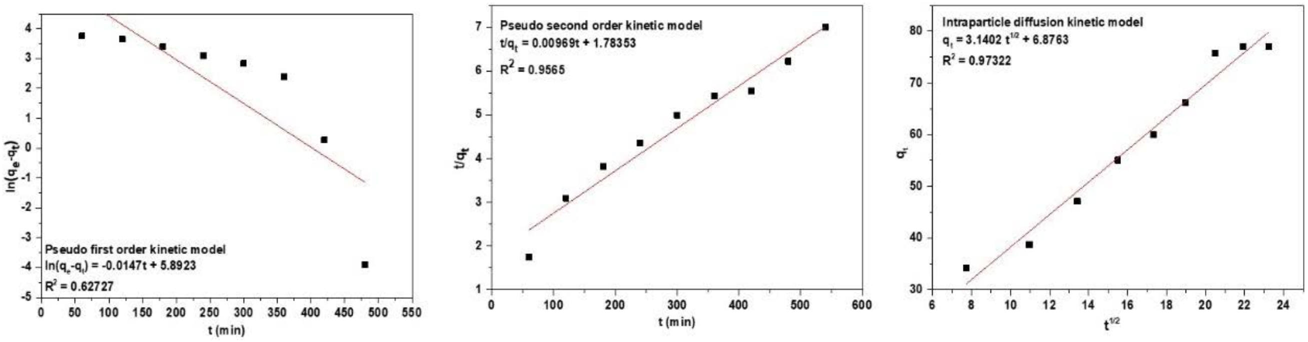

Fig. 9. Plots of studied adsorption kinetic models (a) pseudo-first-order, (b) pseudo-second-order, and (c) interparticle diffusion.

Table 2
Kinetic parameters for the adsorption of Crystal violet obtained through linear regression analysis of various kinetics model

Concentration of dye (mg/L)	Pseudo-first-order			Pseudo-second-order			Interparticle diffusion		
	Q_e	k_1	R^2	Q_e	k_2	R^2	k_i	C	R^2
40	362.23	2.75×10^{-5}	0.63	103.03	5.28×10^{-5}	0.95	3.14	6.87	0.97

Table 3
Thermodynamics parameters for adsorption of Crystal violet

Concentration (mg/L)	Δ*H* (kJ/mol)	Δ*S* (kJ/mol·K)	Δ*G* (kJ/mol) at temperatures					
			303 K	308 K	313 K	318 K	323 K	328 K
40	4,288.77	127.87	–34,455	–35,096	–35,734	–36,374	–37,014	–37,653

Table 4
Parameter of breakthrough curve of adsorptive studies of Crystal violet on *Chenopodium album* bed column

Flow rate (mL/min)	*t* (min)	Peak area (mg·min/L)	q_e (mg/g)	m_{total} (mg/g)	Q_{total} (mg/g)	*R* (%)
2.5	270	267	0.66	3.3	0.33	31.2

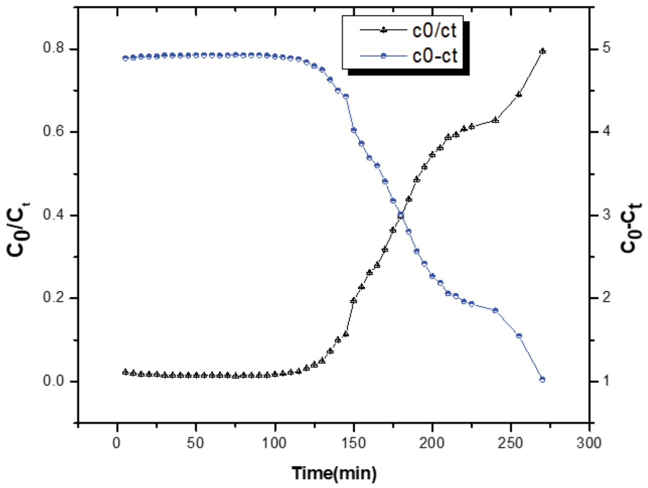

Fig. 11. Breakthrough curve for the adsorption of Crystal violet onto *Chenopodium album* in column operations.

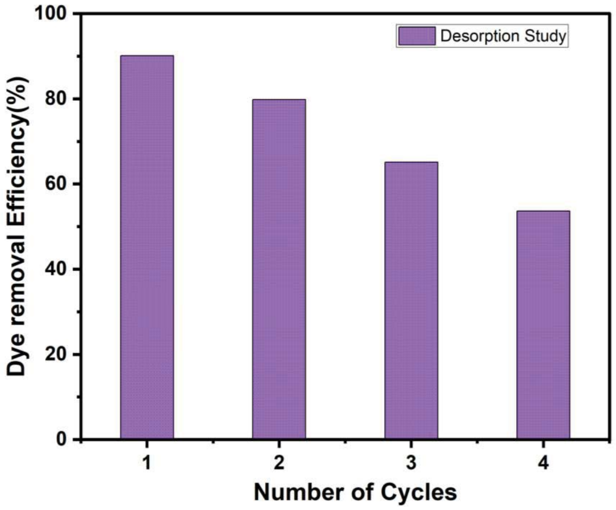

Fig. 12. Desorption study of Crystal violet dye.

temperatures. Adsorption that has positive Δ*H* and Δ*S* values is endothermic and results in a more random adsorbent/adsorbate interaction [53].

3.9. Column adsorption study

Recent studies assess the materials adsorption capability during continuous flow to establish the adsorbents practical application. The procedure was carried out using a column of *C. album* powder at a flow rate of 2.5 mL/min, with a cross-sectional area of 0.8 cm^2, a height of 1 cm, and a mass of 0.5 g. The breakthrough and exhaustion points of the column were determined following the passage of 50 mL of dye solution at C_e/C_0 and were found to be approximately 0.022 and 0.68, respectively (Fig. 11). Using the program OriginPro 8, the curves area under the curve was measured to be 267 cm^2. Table 4's breakdown of the breakthrough parameters shows that the breakthrough limit is much less than the batch capacity. This can be a result of the dye solution's briefer interaction with the *C. album* powder. Only a small amount of adsorbent is sufficient to eliminate a high concentration of CV in a continuous column process [54,55].

3.10. Desorption of adsorbed Methylene blue dye and reusability of C. album adsorbent

The primary objectives of the desorption experiments are adsorbent reusability and sludge management after the sorption phenomena. Reusability of adsorbents in various sorption–desorption cycles is a crucial component for their useful and economical applications. The commercial relevance of adsorbent regeneration and reuse has increased due to the high cost of wastewater purification systems. Adsorbents cause secondary environmental degradation and are expensive for industrial usage if they cannot be employed again or if their adsorption effectiveness is significantly reduced after repeated use. As a result, desorption study of CV (40 mg/L) must be studied. From Fig. 12 it is observed that adsorbent can be used for removal of CV dye up to four consecutive cycles of adsorption–desorption and it removes 53.65% of CV dye.

3.11. Cost estimation

C. album is widely grown weed which can be easily found in many parts of country. In this work we are using fine powder of its aerial part without any further

Table 5
Comparison with other adsorbents for the removal of Crystal violet dye

Adsorbent	C_o (CV) mg/L	Q_e (mg/g)	References
Bottom ash	8	19.40	[3]
Alligator weed	5	15	[15]
Wheat bran	5	15.5	[15]
Laminaria japonica	5	14.5	[15]
Chenopodium album ash powder	40	9.42	[13]
Bagasse fly ash	10	26.23	[56]
Acacia nilotica leaves	40	33	[4]
Jute fiber carbon	50	27.744	[38]
Chenopodium album aerial part	120	219.4	This work

modification for removal of dye which cost negligible and can be prepared easily in laboratory. If cost of transportation and electricity is considered, then also production of adsorbent is negligible when prepared at large scale.

3.12. Comparison study

Table 5 analyses the current investigation's adsorption capability with that of other known adsorbents reported in the literature. The *C. album* weed powder has adsorption capabilities that are comparable to those of other adsorbents. It exhibits the highest CV adsorption capacity among all adsorbents cited in the literature. Even when compared to *C. album* ash powder, the aerial component exhibits greater dye adsorption.

4. Conclusion

The investigations revealed that powder of the aerial part of *C. album* is a robust adsorbent for the removal of CV dye. Effects of various variables, such as contact time, adsorbent dose, pH, temperature, and initial dye concentration were also explored. pH 8 is the ideal pH for the adsorptive removal leading up to 96% removal of the CV at 40 mg/L concentration. The equilibrium of CV dye adsorption was best suited by the greatest coefficient of regression found in the Freundlich and Hill adsorption isotherm. The kinetic study demonstrates that the nature of the adsorption process is endothermic. One of the three kinetics models tested for CV dye, the interparticle diffusion model, offers the best fit. In addition, the experiment fits well with the pseudo-second-order kinetic model. It exemplifies the connection between chemisorption and adsorption. Adsorption takes place spontaneously and favourably at moderate temperatures. Through column testing, it was found that the current adsorbent may be used at an industrial level due to its efficiency in removing 50 ppm of CV solution in just a few hours. Therefore, we can infer that aerial waste of *C. album* is a reliable and cost-effective adsorbent for CV dye.

Acknowledgment

The VRET fellowship provided by the University Grants Commission, New Delhi, India to NR is gratefully acknowledged.

References

[1] A. Saeed, M. Sharif, M. Iqbal, Application potential of grapefruit peel as dye sorbent: kinetics, equilibrium and mechanism of Crystal violet adsorption, J. Hazard. Mater., 179 (2010) 564–572.

[2] D.C. Roy, S.K. Biswas, A.K. Saha, B. Sikdar, M. Rahman, A.K. Roy, Z.H. Prodhan, S.S. Tang, Biodegradation of Crystal violet dye by bacteria isolated from textile industry effluents, Peer J., 6 (2018) e5015, doi: 10.7717/peerj.5015.

[3] A. Mittal, J. Mittal, A. Malviya, D. Kaur, V.K. Gupta, Adsorption of hazardous dye Crystal violet from wastewater by waste materials, J. Colloid Interface Sci., 343 (2010) 463–473.

[4] A.L. Prasad, T. Santhi, Adsorption of hazardous cationic dyes from aqueous solution onto *Acacia nilotica* leaves as an eco-friendly adsorbent, Sustainable Environ. Res., 22 (2012) 113–122.

[5] S. Senthilkumaar, P. Kalaamani, C.V. Subburaam, Liquid phase adsorption of Crystal violet onto activated carbons derived from male flowers of coconut tree, J. Hazard. Mater., B, 136 (2006) 800–808.

[6] J.X. Yu, J. Zhu, L.Y. Feng, X.L. Cai, Y.F. Zhang, R.C. Yu, Removal of cationic dyes by modified waste biosorbent under continuous model: competitive adsorption and kinetics, Arabian J. Chem., 12 (2019) 2044–2051.

[7] A. Mittal, L. Kurup, V.K. Gupta, Use of waste materials-bottom ash and de-oiled soya, as potential adsorbents for the removal of amaranth from aqueous solutions, J. Hazard. Mater., 117 (2006) 171–178.

[8] J. Mittal, D. Jhare, H. Vardhan, A. Mittal, Utilization of bottom ash as a low-cost sorbent for the removal and recovery of a toxic halogen containing dye eosin yellow, Desal. Water Treat., 52 (2014) 4508–4519.

[9] J. Mittal, A. Mittal, Hen Feather: A Remarkable Adsorbent for Dye Removal, S.K. Sharma, Ed., Green Chemistry for Dyes Removal from Wastewater, Scrivener Publishing LLC, USA, 2015, pp. 409–457, doi: 10.1002/9781118721001.ch11.

[10] A. Mittal, M. Teotia, R.K. Soni, J. Mittal, Applications of eggshell and eggshell membrane as adsorbents: a review, J. Mol. Liq., 223 (2016) 376–387.

[11] A. Mittal, R. Ahmad, I. Hasan, Adsorption of Cr(VI) and Cd(II) on chitosan grafted polyaniline-OMMT nanocomposite, Desal. Water Treat., 58 (2017) 144–153.

[12] G. Sharma, Mu. Naushad, D. Pathania, D. Mittal, G.E. Desoky, Modification of *Hibiscus cannabinus* fiber by graft copolymerization: application for dye removal, Desal. Water Treat., 54 (2015) 3114–3121.

[13] C. Arora, D. Sahu, D. Bharti, V. Tamrakar, S. Soni, S. Sharma, Adsorption of hazardous dye Crystal violet from industrial waste using low-cost adsorbent *Chenopodium album*, Desal. Water Treat., 167 (2019) 324–332.

[14] H. Daraeia, A. Mittal, Investigation of adsorption performance of activated carbon prepared from waste tire for the removal of methylene blue dye from wastewater, Desal. Water Treat., 90 (2017) 294–298.

[15] Mu. Naushad, A.A. Ansari, J. Wang, X. Guo, Adsorption isotherm models: classification, physical meaning, application and solving method, Chemosphere, 258 (2020) 127279, doi: 10.1016/j.chemosphere.2020.127279.

[16] Y. Anjaneyulu, N.C. Sreedhara, D.S. Suman Raj, Decolourization of industrial effluents –available methods and emerging technologies – a review, Rev. Environ. Sci. Bio/Technol., 4 (2005) 245–273.

[17] P. Nigam, G. Armou, I.M. Banat, D. Singh, R. Marchant, Physical removal of textile dyes and solid-state fermentation of dye-adsorbed agricultural residues, Bioresour. Technol., 72 (2000) 219–226.

[18] M. Massoudinejad, H. Rasoulzadeh, M. Ghaderpoori, Magnetic chitosan nanocomposite: fabrication, properties, and optimization for adsorptive removal of Crystal violet from aqueous solutions, Carbohydr. Polym., 206 (2019) 844–853.

[19] B.C.S. Ferreira, F.S. Teodoro, A.B. Mageste, L.F. Gil, R.P. de Freitas, L.V.A. Gurgel, Application of a new carboxylate-functionalized sugarcane bagasse for adsorptive removal of

Crystal violet from aqueous solution: kinetic, equilibrium and thermodynamic studies, Ind. Crops Prod., 65 (2015) 521–534.

[20] H.K. Mahilary, A.K. Dey, Preparation and application of carboxylated and mechanically attrited carbon for adsorptive removal of Crystal violet dye, Environ. Sci. Water Res. Technol., 9 (2023) 861–882.

[21] S.H. Vithalkar, R.M. Jugade, Adsorptive removal of Crystal violet from aqueous solution by cross-linked chitosan coated bentonite, Mater. Today: Proc., 29 (2020) 1025–1032.

[22] J. Mittal, R. Ahmad, M.O. Ejaz, A. Mariyam, A. Mittal, A novel, eco-friendly bio-nanocomposite (Alg-Cst/Kal) for the adsorptive removal of Crystal violet dye from its aqueous solutions, Int. J. Phytorem., 24 (2022) 796–807.

[23] P. Pengthamkeerati, T. Satapanajaru, N. Chatasatapattayakul, P. Chairattanamanokom, N. Sananwai, Alkaline treatment of biomass fly ash for reactive dye removal from aqueous solution, Desalination, 261 (2010) 34–40.

[24] M. Mobarak, E.A. Mohamed, A.Q. Selim, M.F. Eissa, M.K. Seliem, Experimental results and theoretical statistical modelling of malachite green adsorption onto MCM-41 silica/rice husk composite modified by beta radiation, J. Mol. Liq., 273 (2019) 68–82.

[25] S.D. Gisi, G. Lofrano, M. Grassi, M. Notarnicola, Characteristics and adsorption capacities of low-cost sorbents for wastewater treatment: a review, Sustainable Mater. Technol., 9 (2016) 10–40.

[26] K.D. Zhang, F.C. Tsai, N. Ma, Y. Xia, H.L. Liu, X.Q. Zhan, X.Y. Yu, X.Z. Zeng, T. Jiang, D. Shi, C.J. Chang, Adsorption behaviour of high stable Zr-based MOFs for the removal of acid organic dye from water, Materials, 10 (2017) 205, doi: 10.3390/ma10020205.

[27] A. Mohamed, S. Yousef, M.A. Abdelnaby, T. Osman, B. Hamawandi, M. Toprak, M. Muhammed, A. Uheida, Photocatalytic degradation of organic dyes and enhanced mechanical properties of PAN/CNTs composite nanofibers, Sep. Purif. Technol., 182 (2017) 219–223.

[28] S. Kuriakos, B. Satpati, S. Mohapatra, Highly efficient photocatalytic degradation of organic dyes by Cu doped ZnO nanostructures, Phys. Chem. Chem. Phys., 17 (2015) 25172–25181.

[29] M. Pourgholi, R.M. Jahandizi, M. Miranzadeh, O.H. Beigi, S. Dehghan, Removal of dye and cod from textile wastewater using AOP (UV/O_3, UV/H_2O_2, O_3/H_2O_2 and $UV/H_2O_2/O_3$), J. Environ. Health Sustainable Dev., 3 (2018) 630–636.

[30] V. Tamrakar, D. Arora, C. Arora, Phytochemical Screening, proximate and elemental analysis of plant species *Curcuma caesia*, *Curcuma longa* and *Chenopodium album*, Res. J. Chem. Environ., 23 (2019) 113–117.

[31] N. Yadav, N. Vasudeva, H.S. Singh, S.K. Sharma, Medicinal properties of genus *Chenopodium* Linn, Nat. Prod. Radiance, 6 (2007) 131–134.

[32] P. Kumar, S. Kumar, Phytochemistry traditional uses, pharmacology of Indian medicinal plant *Chenopodium album* (Linn), World J. Pharm. Pharm. Sci., (2015) 404–421.

[33] A. Nagababu, G.V. Krishna Mohan, K. Ravindranath, Removal of chromium(VI) from polluted water using adsorbents derived from *Chenopodium album* and *Eclipta prostate* plant materials, Int. J. Chemtech. Res., 9 (2016) 506–516.

[34] A. Poonia, A. Upadhyay, *Chenopodium album* Linn: review of nutritive value and biological properties, J. Food Sci. Technol., 52 (2015) 3977–3985.

[35] M.Y. Agrawal, Y.P. Agrawal, P.B. Shamkuwar, Phytochemical and biological activities of *Chenopodium album*, Int. J. Pharm. Technol. Res., 6 (2014) 383–391.

[36] C. Arora, S. Soni, S. Sahu, J. Mittal, P. Kumar, P.K. Bajpai, Iron based metal-organic framework for efficient removal of methylene blue dye from industrial waste, J. Mol. Liq., 284 (2019) 343–352.

[37] S. Soni, N. Rai, P.K. Bajpai, J. Mittal, C. Arora, Enhanced sequestration of an acidic dye on novel bimetallic metal-organic framework, J. Dispersion Sci. Technol., (2022) 1–10.

[38] K.V. Kumar, Linear and non-linear regression analysis for the sorption kinetics of methylene blue onto activated carbon, J. Hazard. Mater., B, 137 (2006) 1538–1544.

[39] H. Shahbeig, N. Bajngheri, S.A. Ghorbanian, A. Hallajisani, S. Poorkarimi, A new adsorption isotherm model of aqueous solutions on granular activated carbon, World J. Modell. Simul., 9 (2013) 243–254.

[40] I. Langmuir, The adsorption of gases on plane surfaces of glass, mica, and platinum, J. Am. Chem. Soc., 40 (1981) 1361–1403.

[41] P. Monash, G. Pugazhenthi, Adsorption of Crystal violet dye from aqueous solution using mesoporous materials synthesized at room temperature, Adsorption, 15 (2009) 390–405.

[42] D. Ringot, B. Lerzy, K. Chaplain, J.P. Bonhoure, E. Auclair, Y. Larondelle, *In-vitro* biosorption of ochratoxin A on the yeast industry by-products: comparison of isotherm models, Bioresour. Technol., 98 (2007) 1812–1821.

[43] S. Soni, P.K. Bajpai, D. Bharti, J. Mittal, C. Arora, Removal of Crystal violet from aqueous solution using iron-based metal-organic framework, Desal. Water Treat., 205 (2020) 386–399.

[44] M.B. Desta, Batch sorption experiments: Langmuir and Freundlich isotherm studies for the adsorption of textile metal ions onto teff straw (*Eragrostis tef*) agricultural waste, J. Thermodyn., 2013 (2013) 375830, doi: 10.1155/2013/375830.

[45] N. Ayawei, A.N. Ebelegi, Modelling and interpretation of adsorption isotherms, J. Chem., 2017 (2017) 3039817, doi: 10.1155/2017/3039817.

[46] K. Foo, B. Hameed, Insights into the modeling of adsorption isotherm systems, Chem. Eng. J., 156 (2010) 2–10.

[47] X. Han, X. Niu, X. Ma, Adsorption characteristics of methylene blue on poplar leaf in batch mode: equilibrium, kinetics, and thermodynamics, Korean J. Chem. Eng., 29 (2012) 494–502.

[48] M. Iqbal, A. Saeed, S.I. Zafar, FTIR spectrophotometry, kinetics and adsorption isotherms modelling, ion exchange, and EDX analysis for understanding the mechanism of Cd^{2+} and Pb^{2+} removal by mango peel waste, J. Hazard. Mater., 164 (2009) 161–171.

[49] L. Qiang, B. Chen, P. Lin, J. Zhou, J. Zhan, Q. Shen, X. Pan, Adsorption of heavy metal from aqueous solution by dehydrated root powder of long-root *Eichhornia crassipes*, Int. J. Phytorem., 18 (2016) 103–109.

[50] H.B. Hameed, D.K. Mahmoud, A.L. Ahmad, Equilibrium modelling and kinetic studies on the adsorption of basic dye by a low-cost adsorbent: coconut (*Cocos nucifera*) bunch waste, J. Hazard. Mater., 158 (2008) 65–72.

[51] H.K. Jayasantha, P. Krishnamoorthy, T.K. Arumugam, S. Radhakrishnan, D. Vasudevan, An efficient removal of Crystal violet dye from wastewater by adsorption onto TLAC/chitosan composite: a novel low-cost adsorbent, Int. J. Biol. Macromol., 96 (2017) 324–333.

[52] M. Ghasemi, Mu. Naushad, N. Ghasemi, Y.F. Khosravi, A novel agricultural waste-based adsorbent for the removal of Pb(II) from aqueous solution: kinetics, equilibrium, and thermodynamic studies, J. Ind. Eng. Chem., 20 (2014) 454–461.

[53] Z.A. Alothman, J. Mittal, Synthesis, and characterization of $YVO_4:Eu^{3+}$ nanoparticles: kinetics and isotherm studies for the removal of Cd^{2+} metal ion, Desal. Water Treat., 57 (2016) 2081–2088.

[54] A. Mittal, Mu. Naushad, G. Sharma, Z.A. Alothman, S.M. Wabaidur, M. Alam, Fabrication of MWCNTs/ThO_2 nanocomposite and its adsorption behavior for the removal of Pb(II) metal from aqueous medium, Desal. Water Treat., 57 (2016) 21863–21869.

[55] M.A. Abuh, G.K. Akpomie, N.K. Nwagbara, A.N. Bassey, D.I. Ape, B.U. Ayabi, Kinetic rate equations application on the removal of copper(II) and zinc(II) by unmodified lignocellulosic fibrous layer of palm tree trunk-single component system studies, Int. J. Basic Appl. Sci., 1 (2013) 800–809.

[56] I.D. Mall, V.C. Srivastava, N.K. Agarwal, Removal of Orange-G and Methyl Violet dyes by adsorption onto bagasse fly ash—kinetic study and equilibrium isotherm analyses, Dyes Pigm., 69 (2006) 210–223.